Sequence-Based Design and Discovery of Peptide Inhibitors of HIV-1 Integrase: Insight into the Binding Mode of the Enzyme

Hui-Yuan Li,[†] Zahrah Zawahir,[‡] Lai-Dong Song,[†] Ya-Qiu Long,*[,†] and Nouri Neamati*[,‡]

State Key Laboratory of Drug Research, Shanghai Institute of Materia Medica, Shanghai Institutes for Biological Sciences, Graduate School of the Chinese Academy of Sciences, CAS, 555 Zuchongzhi Road, Shanghai 201203, China, and the Department of Pharmaceutical Sciences, School of Pharmacy, University of Southern California, 1985 Zonal Avenue, Los Angeles, California 90089

Received March 16, 2006

Integration of viral DNA into the host chromosome is an essential step in the HIV life cycle. This process is mediated by integrase (IN), a 32 kDa viral enzyme that has no mammalian counterpart, rendering it an attractive target for antiviral drug design. Herein, we present a novel approach toward elucidating "hot spots" of protein−protein or protein−nucleic acid interactions of IN through the design of peptides that encompass conserved amino acids and residues known to be important for enzymatic activity. We designed small peptides (7−17 residues) containing at least one amino acid residue that is important for IN catalytic activities (3′-processing and strand transfer) or viral replication. All these peptides were synthesized on solid phase by fluorenylmethoxycarbonyl (Fmoc) chemistry and evaluated for their inhibition of IN catalytic activities. Such specific sites of interest (i.e., protein−DNA or protein−drug interactions) could potentially be used as drug targets. This novel "sequence walk" strategy across the entire 288 residues of IN has allowed the identification of two peptides NL-6 and NL-9 with 50% inhibitory concentration (IC_{50}) values of 2.7 and 56 μM for strand transfer activity, respectively. Amino acid substitution analysis on these peptides revealed essential residues for activity, and the rational truncation of NL-6 produced a novel hexapeptide (peptide NL6-5) with inhibitory potency equal to that of the parent dodecapeptide (peptide NL-6). More significantly, the retroinverso analogue of NL-6 (peptide RDNL-6) in which the direction of the sequence is reversed and the chirality of each amino acid residue is inverted displayed improved inhibitory potency against 3′-processing of HIV-1 IN by 6-fold relative to the parent NL-6, serving as a metabolically stable derivative for further in vitro and in vivo analyses.

Introduction

HIV-1 integrase (IN) is essential for viral replication. Following reverse transcription of the RNA into DNA by HIV-1 reverse transcriptase, IN integrates the viral DNA into the host genome. IN performs its catalysis in two steps: 3′-processing and strand transfer. Initially, it cleaves the viral DNA ends at the highly conserved CAGT site to release a GT dinucleotide in the cytoplasm.[1−3] IN subsequently transfers the viral DNA into the host chromosome in the nucleus. Successful integration requires the interaction of IN with other viral and host cell proteins including, but not limited to, LEDGF, thought to be involved in nuclear translocation of the preintegration complex; BAF, thought to prevent autointegration of viral DNA; and Rad18 and Poly (ADP-ribose) polymerase, which are among a group of repair enzymes thought to interact with IN during DNA repair and ligation following the integration process (for a recent review see ref 4). The viral reverse transcriptase protein is also thought to interact with IN in the preintegration complex.[5]

Specific regions of IN are known to be essential for catalytic function.[6] Analogously, there exist specific regions on the enzyme that are required for distinct protein−protein and protein−DNA interactions that are critical for efficient integration. Binding and catalytic activity assays of rationally designed peptides against targeted proteins should provide a unique tool toward elucidating, at a molecular level, important biochemical sites of the enzyme. In this study, we have defined possible regions of IN involved in catalysis at the amino acid level. In particular, sequences derived from the α1 helix and the α3 helix of IN appear to play an important role in binding to the enzyme and interrupting its catalytic activity.[7] Our unpublished data suggest that these peptides are size-dependent, as longer peptides containing the same residues show differences in the inhibition of catalytic activity.

The success of developing protease inhibitors is based on rational design of peptidic and peptidomimetic compounds with high selectivity. Although numerous small-molecule inhibitors of IN are known, peptide-based approaches targeting IN have been very limited. The first and most elegant study in this respect was reported by Plasterk et al. who identified a hexapeptide inhibitor of IN by using a combinatorial peptide library.[8] They screened a synthetic library of potentially 400 000 hexapeptides and identified a lead peptide with the sequence HCKFWW that inhibited IN-mediated 3′-processing and integration with an IC_{50} of 2 μM.[8] This peptide also inhibited HIV-2, FIV, and MLV integrases, suggesting that a conserved region of IN is targeted. They suggested that HCKFWW acts at or near the catalytic site of IN. It has also been reported that a short peptide identified from a yeast genomic library inhibits IN catalytic activity by interfering with IN−DNA binding.[9] A more recent study used phage-display techniques to identify a novel peptide that selectively inhibited the strand transfer activity of IN.[10] In addition, 10-mer long peptides deriving from the reverse transcriptase region also inhibit IN catalytic activity.[11] Other inhibitory peptides of IN targeting catalytic activity as well as protein oligomerization, although far from entering actual drug development, have since been reported. Maroun et al. showed that a peptide reproducing the α5 dimerization helix sequence

* To whom correspondence should be addressed. For Y.-Q.L.: phone, 86-21-50806876; fax, +86-21-50806876; e-mail: yqlong@mail.shcnc.ac.cn. For N.N.: phone, 323-442-2341; fax, 323-442-1390; e-mail, neamati@usc.edu.
[†] Shanghai Institutes for Biological Sciences.
[‡] University of Southern California.

10.1021/jm060307u CCC: $33.50
Published on Web 06/29/2006

Table 1. Catalytic and Replication Activities of a Series of Integrase Mutants

sequence[a]	segment	mutation	3′-pr[b,f]	integ[c,f]	disint[d,f]	repl (infect)[e,f]
EE**H**EKY**H**SNW	10−19	H12A	+	+	+++	−
		H16A			+++	−
AS**C**DKCQLKG	38−47	C40A	−	−	+++	−
		C43A	+	+	+++	−
HGQVD**C**SPGIWQL**DCT**H	51−67	H51A				+
		D64A	−	−	−	−
		T66A	+	+	+++	+
VHVA**S**GY	77−83	S81A	+/−	+/−	+/−	−
PA**E**TGQET	90−97	E92A	++	++	++	++
TAYFLLKLAGRW	97−108					
GRW**P**VKT	106−112	P109A	+/−	+/−	−	+
HT**DN**GSNF	114−121	D116	−	−	−	−
		N117S	+	+	+	
		F121A	+/−	−		
ACWWAG**IK**QEF	129−139	I135P				−
		K136A	+/−	+/−	+++	−
FGIP**Y**NPQ**S**Q	139−148	Y143N	+++		+++	delayed
		S147I	−		+++	−
ESMNKELKKI	152−161	E152A	−	−	−	−
		S153A	+	+	+++	+++
V**R**DQAEHLKT	165−175	R166A				−
FIHN**F**KRK	181−188	F185A	+++	+++		−
GYSAGE**R**IVD	193−202	R199A	+++	+++	+++	−
WKGPAK**LL**WK	235−244	W235A	+++	+++	+++	+/−
		L241A	−	−	−	
		L242A	−	−	+	
VP**RR**KAKI	260−267	V260E	−	−	−	
		R262G	++	++	+	
		R263L	++	++	++	

[a] The residues in bold are important for HIV-1 integrase catalytic activity in vitro and effective viral replication. [b] 3′-Processing. [c] Integration (strand transfer). [d] Disintegration. [e] Replication or infectivity capability. Notations: (−) 0−10% activity of the wild-type enzyme; (+) 10−40%; (++) 40−80%; (+++) 80−100%.

Scheme 1. Synthetic Scheme for Fmoc-Based Solid-Phase Preparation of NL-1

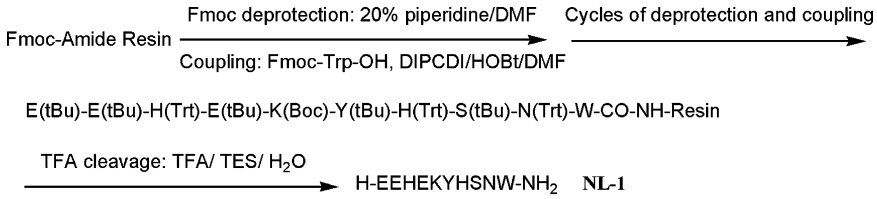

of IN inhibits catalytic activity, as does a peptide with the α1 helix sequence, albeit at a higher micromolar concentration.[7] Another study that screened peptides derived from the dimerization interface of IN also shows similar results and indicates that interaction of such peptides with the enzyme may block its dimerization.[12] Finally, it has been shown that a 30-mer peptide from residues 147−175 of IN inhibited catalytic activity at low millimolar concentrations. This study also suggested that conformational analysis of peptides derived from IN will allow the development of peptidomimetic and other inhibitors against IN.[13] Although several larger peptides derived from other sources have been reported to inhibit IN in vitro, no other study thus far has attempted to systematically and rationally design small-peptide inhibitors of IN.[14] Also reported are peptide inhibitors targeting other aspects of the HIV-1 life cycle, including T-20 (a fusion inhibitor) and a capsid assembly inhibitor, targeting the assembly of capsid particles in vitro.[15,16]

In an effort to take advantage of a growing list of studies defining the role of particular amino acid residues in catalysis and DNA binding (Table 1, for a review see refs 17 and 18), we designed a series of small peptides, each of which contained at least one amino acid residue important for IN catalytic activities and/or viral replication. Our approach is based on the sequence of HIV-1 IN to explore the mechanism of integration and DNA and drug binding and to provide a new pharmacophore for antiviral design and development. With this approach it may be possible to find the Achilles heel of the enzyme that might be important for the development of drug resistance and to discover a novel site that could be used to develop inhibitors. These peptides, in addition to interfering with HIV-1 IN catalytic activity, may also disrupt HIV-1 infectivity, and thus serve as

Table 2. Sequence and HIV-1 Integrase Inhibitory Activity of the Designed Peptides

code	sequence	fragment	3′-processing IC_{50}, μM	strand transfer IC_{50}, μM
	N-Terminus Region			
NL1	EEHEKYHSNW	10−19	>2000	>2000
NL2	ASCDKCQLKG	38−47	>2000	>2000
NL3	HGQVDCSPGIWQLDCTH	51−67	1000	1000
NL4	VHVASGY	77−83	>2000	>2000
NL5	PAETGQET	90−97	>2000	>2000
NL-6	TAYFLLKLAGRW	97−108	**21 ± 7**	**2.7 ± 1**
NL7	GRWPVKT	106−112	>2000	>2000
NL8	HTDNGSNF	114−121	>2000	>2000
	Catalytic Core Region			
NL-9	ACWWAGIKQEF	129−139	**95 ± 9**	**56 ± 5**
NL10	FGIPYNPQSQ	139−148	>1000	>1000
NL11	ESMNKELKKI	152−161	>2000	>2000
NL12	VRDQAEHLKT	165−175	>2000	>2000
NL13	FIHNFKRK	181−188	>2000	>2000
NL14	GYSAGERIVD	193−202	>2000	>2000
NL15	WKGPAKLLWK	235−244	>1000	>1000
	C-Terminus Region			
NL16	VPRRKAKI	260−267	>1000	>1000

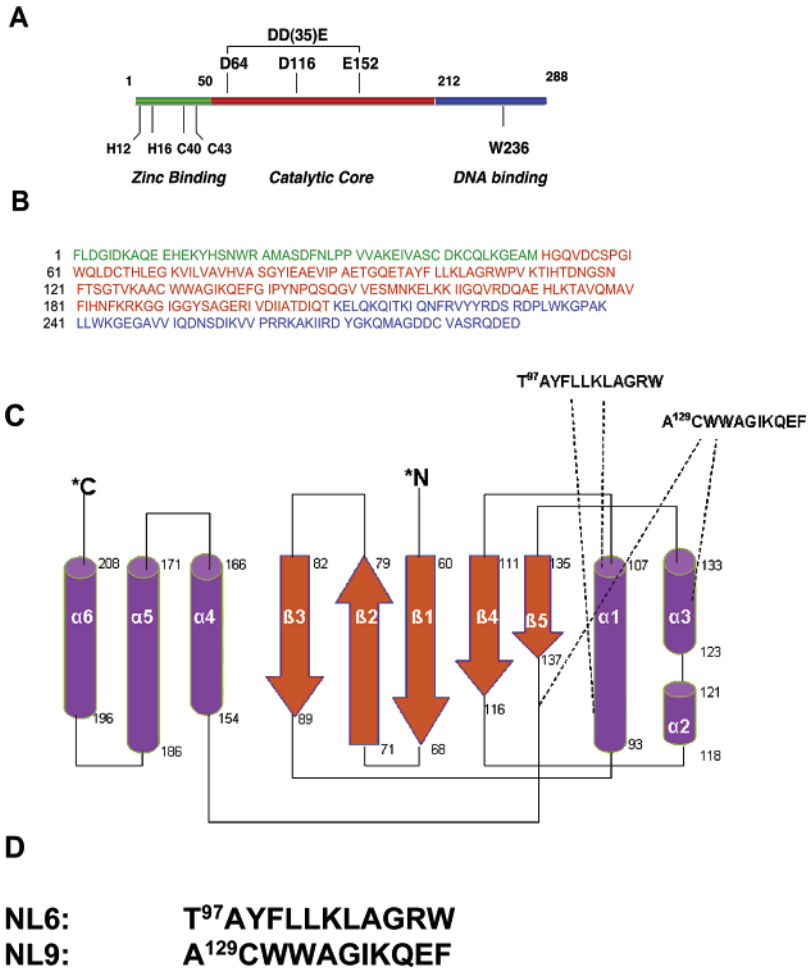

Figure 1. Three functional motifs of HIV-1 IN. (A) The N-terminus shown in green contains the highly conserved HHCC motif that binds to zinc. The catalytic core shown in red contains the highly conserved DDE motif that binds to divalent metals. The least conserved C-terminus shown in blue binds to DNA. (B) Sequence of the full-length HIV-1 integrase. (C) The secondary structure of IN. The peptides with the best inhibitory activity show sequences derived from the α1 helix (NL6) and part of the α3 helix (NL9). (D) Sequences of the lead peptides NL6 and NL9.

possible leads for peptidomimetic prodrugs against the virus. In this study, the design, synthesis, and evaluation of these small peptides including amino acid substituted and truncated analogues as IN inhibitors are reported. We have discovered that certain amino acid residues are key in the inhibitory potential of these peptides and may also be implicated in IN catalytic activity. Furthermore, conformational requirements were also explored with respect to the inversion and retroinversion of the peptide sequences, providing a better understanding of the mode of IN inhibitory action by these new agents.

Results

Using the general method presented in Scheme 1, we prepared a series of sequence-based small peptides. As shown in Table 2, our designed peptides cover the entire functional domains of IN (Figure 1). Two peptides show selective inhibitory activity against wild-type IN: NL-6, corresponding to residues 97−108 of IN, and NL-9, corresponding to residues 129−139 of IN. Figure 1C shows the location of these peptides on the enzyme. The structures of these two peptides and their positions on the IN crystal structure (PDB 1K6Y) are shown in Figure 2.

Activity of Sequence-Based Peptides. Inhibition of IN specific catalytic activities were carried out by monitoring both the DNA cleavage step (3′-processing) and the DNA strand transfer (integration). Our initial sequence-directed peptide library indicated that the methodology we employed for the design of IN inhibitors on the basis of the amino acid sequence of IN is encouraging. Among the 16 synthesized peptides, two compounds, NL-6 and NL-9, exhibited promising IN inhibitory activity with IC_{50} values of 21 ± 7 and 95 ± 9 μM for 3′-processing and 2.7 ± 1 and 56 ± 5 μM for integration, respectively (Table 2), even though the other 14 peptides did not show obvious inhibitory activity toward IN. This finding suggests that the two segments of NL-6 and NL-9 might be selectively targeting IN. On the basis of the two lead peptides (Figure 2), further structural modifications were carried out to provide high-affinity IN inhibitors and to furnish information on IN topography concerning the bound conformation of the inhibitor.

Alanine Scanned Analogues of NL-6 and NL-9. We synthesized alanine-substituted mutations of NL-6 and NL-9 to explore the functional importance of the constituent amino acid residues in the two peptides. The activity data (Table 3) indicate that Y^3, F^4, L^6, L^8, and W^{12} are the essential residues in NL-6, whose deletion resulted in a significant loss of the IN inhibitory activity. The loss of activity for NL-6 F4A, L6A, L8A, and W12A were >17-fold for 3′-processing and >120-fold for strand transfer. For the NL-9 peptide, residues C^2, W^4, I^7, Q^9, E^{10}, and F^{11} are each vital for the inhibition of the IN. These residues might be involved in the direct contact in binding the surface of the enzyme. However, an interesting result is observed when substituting the Trp3 with an Ala residue. The 3′-processing and strand transfer inhibitory activity of the peptide were both increased by 4-fold (IC_{50} = 23 ± 6 μM) and 2.3-

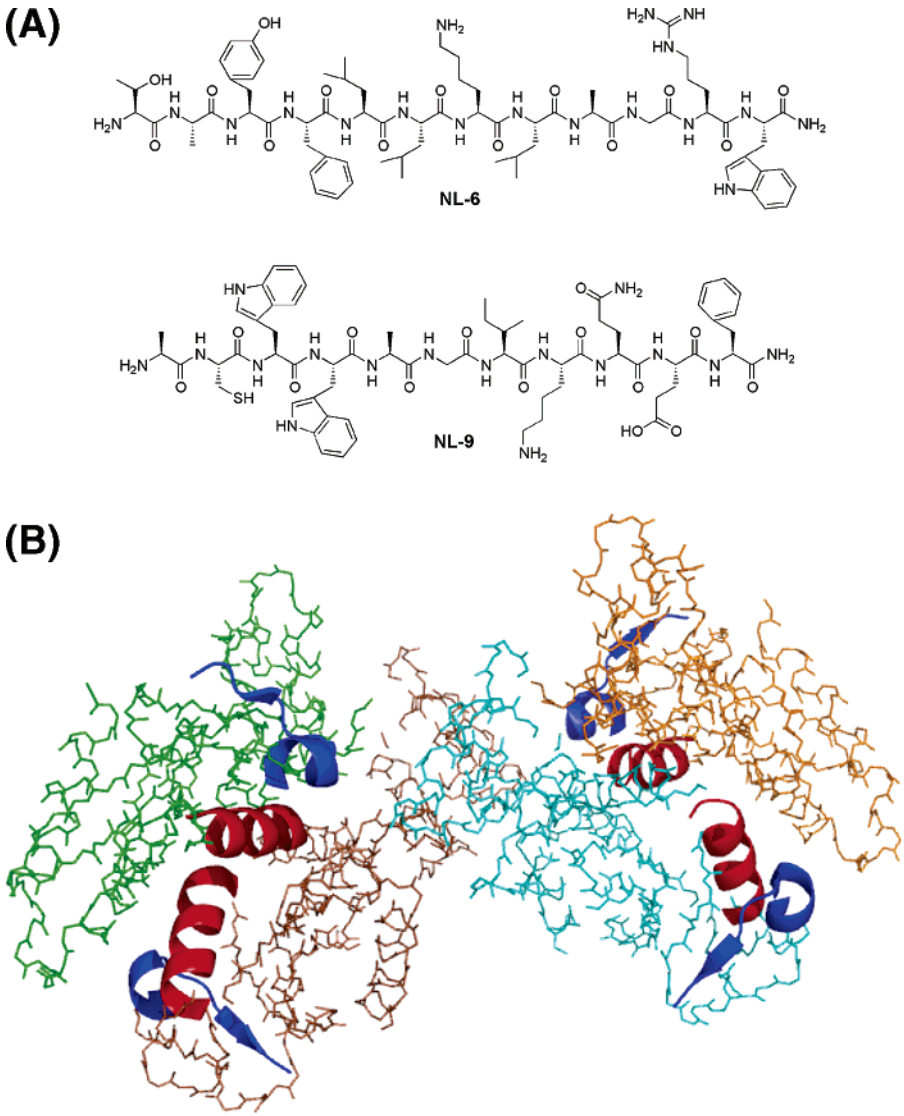

Figure 2. Chemical structures of the lead compounds NL-6 and NL-9 (A) and their positions on HIV-1 IN (B). The most potent peptides (red, NL-6, and blue, NL-9) are shown in the context of four identical tetramers (green, brown, cyan, orange) of the IN N-terminal domain and the catalytic core domain (PDB 1K6Y).

fold (IC_{50} = 24 ± 8 μM), respectively relative to the parent peptide NL-9. Substitution of Trp4 with an Ala has the opposite effect: inhibitory activity is completely abolished for both integration and strand transfer. The same result occurs with the Trp3 and Trp4 substitutions for other amino acids in the single-substituted analogues of NL-9. Figure 3 shows the results of NL9-W4A and NL9-W3A substitutions in comparison with the parent peptide.

Single Substituted Analogues of NL-6 and NL-9. With the identification of essential amino acids in NL-6 and NL-9 through alanine scanning, we chose Y^3, K^7, and W^{12} of NL-6 and we chose C^2, W^3, W^4, and K^8 of NL-9 to make several additional substitutions to determine what structural feature of the side chain is favored for the inhibition of IN. Therefore, during this second stage of the structure−activity study, single-substituted analogues were synthesized and evaluated for their IN inhibitory activity. The biological data are summarized in Table 4. Our results indicate that both the tyrosine and tryptophan residues in NL-6 are important in maintaining IN inhibitory activity. When the tyrosine residue is substituted by serine, the IC_{50} values were found to be 186 ± 23 μM for 3′-processing and 11 ± 2 μM for integration. Replacement by a leucine of the tryptophan residue produced IC_{50} values of 315 ± 30 and 38 ± 2 μM for 3′-processing and integration, respectively. This is a 6-fold loss in catalytic activity. However, when the lysine residue was substituted by isoleucine, the potency was increased 3-fold, suggesting that the side chain in this position might be directed into a hydrophobic region on the binding surface of the IN. With respect to NL-9, an ACWW motif proved essential for maintaining the IN activity. Substitution of cysteine by serine showed IC_{50} values of 294 ± 41 and 163 ± 15 μM for 3′-processing and integration, respectively, while replacement of one of the tryptophan residues (Trp4) with glycine resulted in a total loss of the IN inhibitory activity (Table 4). Arginine substitution for lysine also caused remarkable activity loss. These preliminary results suggest that the basic residues, e.g., Lys and Arg, and the Trp in common between NL-6 and NL-9 might be important for the functional interactions. Interestingly, similar to the alanine scanning results, substitution of Trp3 with glycine resulted in a 2-fold increase in IN inhibitory activity compared to the parent peptide.

Truncated Analogues of NL-6 and NL-9. Further structure−activity studies were conducted on NL-6 and NL-9 to determine the minimal sequence required for inhibitory activity against IN. As shown in Table 5, NL-6 was truncated into three hexamers (NL6-4, NL6-5, and NL6-6). Interestingly, the core

Table 3. HIV-1 Integrase Inhibitory Activity of the Alanine Scanned Analogues of NL-6 and NL-9

compd	sequence	3′-processing IC_{50}, μm	strand transfer IC_{50}, μm
NL-6	TAYFLLKLAGRW	21 ± 7	2.7 ± 1
NL6-T1A	AAYFLLKLAGRW	100 ± 10	47 ± 7
NL6-Y3A	TAAFLLKLAGRW	193 ± 10	119 ± 11
NL6-F4A	TAYALLKLAGRW	>333	>333
NL6-L5A	TAYFALKLAGRW	115 ± 21	51 ± 7
NL6-L6A	TAYFLAKLAGRW	>333	>333
NL6-K7A	TAYFLLALAGRW	113 ± 15	56 ± 7
NL6-L8A	TAYFLLKAAGRW	>333	106 ± 7
NL6-G10A	TAYFLLKLAARW	118 ± 10	19 ± 6
NL6-R11A	TAYFLLKLAGAW	83 ± 15	80 ± 8
NL6-W12A	TAYFLLKLAGRA	>333	>333
NL 9	ACWWAGIKQEF	95 ± 9	56 ± 5
NL9-C2A	AAWWAGIKQEF	277 ± 47	311 ± 19
NL9-W3A	ACAWAGIKQEF	33 ± 6	34 ± 8
NL9-W4A	ACWAAGIKQEF	>333	>333
NL9-G6A	ACWWAAIKQEF	90 ± 10	43 ± 7
NL9-I7A	ACWWAGAKQEF	>333	>333
NL9-K8A	ACWWAGIAQEF	62 ± 13	55 ± 7
NL9-Q9A	ACWWAGIKAEF	>333	>333
NL9-E10A	ACWWAGIKQAF	>333	>333
NL9-F11A	ACWWAGIKQEA	245 ± 13	206 ± 12

Table 4. HIV-1 Integrase Inhibitory Activity of the Single-Substituted Analogues of NL-6 and NL-9

compd	sequence	3′-processing IC_{50}, μm	strand transfer IC_{50}, μm
NL-6	TAYFLLKLAGRW	21 ± 7	2.7 ± 1
NL6-1	TA*S*FLLKLAGRW	186 ± 23	11 ± 2
NL6-2	TAYFLL*I*LAGRW	4.1 ± 0.7	3.0 ± 1.0
NL6-3	TAYFLLKLAGR*L*	315 ± 30	38 ± 2
NL-9	ACWWAGIKQEF	95 ± 9	56 ± 5
NL9-1	A*S*WWAGIKQEF	294 ± 41	163 ± 15
NL9-2	AC*G*WAGIKQEF	46 ± 5	16 ± 2
NL9-3	ACW*G*AGIKQEF	>333	>333
NL9-4	ACWWAGI*R*QEF	>333	>333

sequence NL6-5, i.e., YFLLKL, showed comparable activity with respect to the parent peptide NL-6, which is consistent with the alanine scanning results. The shortened peptide of NL6-5 containing Y^3, F^4, L^6, and L^8 (four key residues out of five) in NL-6 was equally potent as the dodecamer peptide NL-6. The previous investigation on the alanine mutation showed that the alanine substitution on the residues outside the core sequence of NL-6 resulted in a loss of the inhibitory potency, but the truncated analogue without the residues outside the core sequence still kept the activity. We proposed that the single-substituted analogues might possess a conformation different from that of the truncated one. Since the side chain of the essential residues played an important role in the binding with the protein, the changed structure of the side chain might distort the original conformation of the dodecamer peptide to some extent. For the truncated analogue, the retention of the core sequence might help the retention of active conformation in the absence of the extra residues. However, NL-9 lost all activity when it was truncated into three segments. Only the N-terminal part of NL-9, i.e., peptide NL9−5, bearing the core motif of ACWW is slightly active against the strand transfer of IN.

Conformational Modification of NL-6 and NL-9. The dimeric nature of the catalytic domain of HIV-1 IN suggested that peptides derived from the dimerization interface of the enzyme might function as specific inhibitors of the enzyme by preventing its self-association. It is important to bear in mind that under physiological condition IN may function as a multiple units of a dimer such as tetramer or octamer. Whatever the oligomeric nature of IN might be, the oligomeric enzyme is made of such repeated units and the dimer interface remains

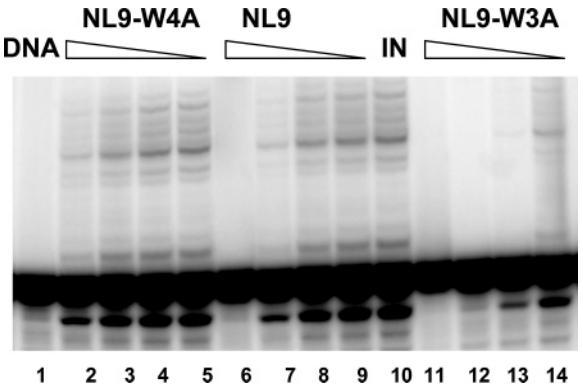

Figure 3. Inhibitory activity of analogues of NL9. Alanine scanned analogues of parent peptide NL9 show a decrease in potency when Trp4 is substituted with Ala and an increase in potency from the parent peptide when Trp3 is substituted: (lane 1) DNA only; (lanes 2−5) 333, 111, 37, 12 μM NL9-4; (lanes 6−9) 333, 111, 37, 12 μM NL9; (lanes 11−14) 333, 111, 37, 12 μM NL9-3; (lane 10) wild-type IN only.

Table 5. HIV-1 Integrase Inhibitory Activity of the Truncated Analogues of NL-6 and NL-9

compd	sequence	3′-processing IC_{50}, μm	strand transfer IC_{50}, μm
NL-6	TAYFLLKLAGRW	21 ± 7	2.7 ± 1
NL6-4	TAYFLL	500	500
NL6-5	YFLLKL	20	20
NL6-6	KLAGRW	>100	> 100
NL-9	ACWWGAKIQEF	95 ± 9	56 ± 5
NL9-5	ACWWAG	>100	60
NL9-6	WAGIKQ	>100	>100
NL9-7	IKQEF	>100	>100

the same. Structural data indicate that the interfacial region of dimeric HIV-1 IN involves strong helix-to-helix contacts α1/α5′ and α5/α1′, where both hydrophobic and electrostatic interactions contribute to dimer stabilization.[19,20] Our active peptides NL-6 and NL-9 fall within the sequence of α1 (residues 95−109) and α3 (residues 123−133), respectively. To explore the conformational requirement, we designed D-peptides composed of all-D amino acid residues of NL-6 and NL-9 (peptides DNL-6 and DNL-9). The retro isomers of NL-6 and NL-9 (peptides RNL-6 and RNL-9) were also synthesized, with the sequence of amino acids from the N- to the C-terminus identical to the sequence of NL-6 and NL-9 reading from the C- to N-terminus. The retroinverso isomers of NL-6 and NL-9 (peptides RDNL-6 and RDNL-9) possess both the direction of the sequence and the chirality of the amino acids opposite those of NL-6 and NL-9. The all-D, retro, and retroinverso peptides belong to a topochemistry, which aims at the change of whole conformation and configuration when the backbone is modified. This serves as a major tool in probing biomolecular topology.[21−23] We synthesized two pairs of enantiomers: the natural peptide and the D-peptide; the retro peptide and the retroinverso analogue. The peptide and its retroinverso isomer are equivalent in topochemistry. The helical propensity of peptides NL-6 and its mirror image isomer, retro isomer, and retroinverso isomer was measured by circular dichroism (CD) with 50 v/v % of 2,2,2-trifluoroethanol (TFE), an α-helix-stabilizing solvent (Figure 4). The CD spectra of these peptides showed the regular Cotton effect. NL-6 and RNL-6 exhibited a positive Cotton effect at 192 nm and a negative Cotton effect at 208 and 222 nm. DNL-6 and RDNL-6 exhibited a negative Cotton effect at 192 nm and a positive Cotton effect at 208 and 222 nm. All the CD spectra showed distinct maxima and minima at 208 and 222 nm, respectively, consistent with induction of an α-helical

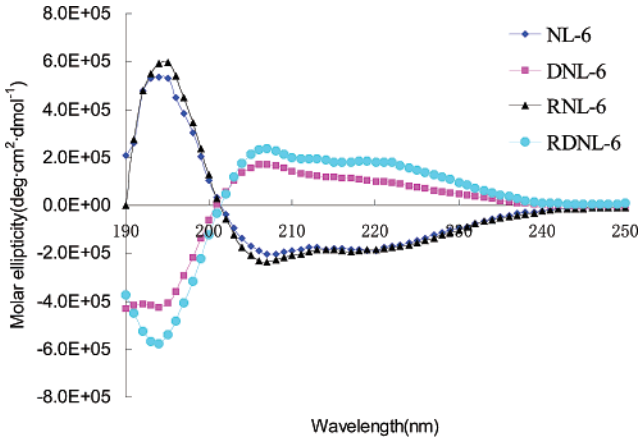

Figure 4. CD spectra of NL-6 (100 μM) and its isomers in 10 mM PBS, pH 7.2, and 50% (v/v) TFE at room temperature.

Table 6. Calculated Content of α-Helix of NL-6 and Its Isomers from CD Data Based on the Method Reported Previously[24]

peptide	% α-helix
NL-6	46
RNL-6	46
DNL-6	25
RDNL-6	47

Table 7. HIV-1 Integrase Inhibitory Activity of the Mirror Image Isomer, Retro Isomer, and Retroinverso Isomer of NL-6 and NL-9

compd	sequence	3′ processing IC_{50}, μm	strand transfer IC_{50}, μm
NL-6	TAYFLLKLAGRW	21 ± 7	2.7 ± 1
DNL-6	tayfllklagrw[a]	65 ± 8	13 ± 1
RNL-6	WRGALKLLFYAT	96 ± 2	16 ± 4
RDNL-6	wrgalkllfyat[a]	3.5 ± 1	4.0 ± 1
NL-9	ACWWAGIKQEF	95 ± 9	56 ± 5
DNL-9	acwwagikqef[a]	>1000	>1000
RNL-9	FEQKIGAWWCA	>1000	>1000
RDNL-9	feqkigawwca[a]	>1000	>1000

[a] Represents D-configured amino acid.

conformation. NL-6 and RNL-6 preferentially form a right-handed α-helix, while DNL-6 and RDNL-6 form a left-handed α-helix, consistent with their enantiomeric relationship. Table 6 shows the calculated percentages of the α-helix forms from the CD data for peptides NL-6, DNL-6, RNL-6, and RDNL-6 in 50% TFE.[24]

We evaluated the inhibitory activity of the isomers against IN. As shown in Table 7, all three isomeric forms of NL-9 completely lost the inhibitory effect compared to the parent peptide (Figure 5A). Conversely, the isomers of NL-6 all show inhibitory activity to varying extents compared to the parent peptide. The D-isomeric form shows a higher micromolar IC_{50} value (96 ± 2 μM) for 3′-processing but an almost 6-fold decrease in IC_{50} value for integration (16 ± 4 μM). In a similar pattern of selectivity for integration, the retro isomer shows an IC_{50} value of 65 ± 8 μM for 3′-processing and 13 ± 1 μM for integration. The retroinverso isomer RDNL-6 has the best IN inhibitory activity with IC_{50} values of 3.5 ± 1 and 4 ± 1 μM for 3′-processing and integration, respectively, showing a 6-fold increase in potency for 3′-processing compared to the parent peptide (Figure 5B, Table 7).

Discussion

HIV-1 IN is a 288-amino acid protein consisting of three functional domains: the N-terminus, the catalytic core, and the C-terminus (Figure 1A,B). Previously we compiled a list of all reported IN mutants and compared their in vitro activities as well as their potential infectivity.[17] On the basis of these results, we wanted to understand the role of each individual amino acid in the context of a 7−17 residue long peptide (a distance of <20Å). Such peptides not only are useful for mapping DNA−protein interactions or protein−protein interactions but also can be used as drug leads. In our initial attempt we designed 16 peptides, each of which contained at least one conserved residue known to reduce the in vitro activity of IN or block viral replication (Table 1). The 16 peptides were synthesized using fluorenylmethoxycarbonyl (Fmoc) chemistry and purified by reverse-phase HPLC. Assays were carried out by monitoring both the nucleotide cleavage and the DNA strand transfer (integration) reactions in an in vitro assay specific for IN (see "Materials and Methods" for methods).

Viruses with amino acid substitutions at conserved residues shown in Table 1 were replication-incompetent. Moreover, several other residues were also identified that were not highly conserved but dramatically reduced IN activities and viral spread (Table 1). The simple explanation could be that these mutated enzymes are not able to recognize and cleave viral DNA. Alternatively, these mutations cause a decrease or disruption of interaction between IN and other viral and cellular proteins. In our effort in elucidating residues important in DNA recognition and enzymatic activity, we applied a novel strategy we call "sequence walk" to identify unique motifs that could potentially be exploited as drug targets.

Peptide NL-6 is derived from the IN enzyme residues 97−108. No IN mutants from this region have thus far been examined for enzymatic activity, HIV-1 infectivity, and replication. From our data, however, it is interesting that single substitutions of certain residues result in a complete loss of inhibitory activity compared to the parent peptide. The NL6-F4A, NL6-L6A, and NL6-W12A substitutions are examples of this event. An interesting and opposite result is obtained with the NL6-K7I substitution: the peptide becomes more potent in inhibiting both catalytic activities. It is possible that this particular residue interrupts DNA binding, and further studies are underway to investigate the implications of the substitutions and to eliminate the possibility of nonspecific binding. With regard to peptide NL-9, spanning residues 129−139 on the enzyme, K136 is known to be important in DNA binding.[25] As expected, significant changes in potency of the peptide occur when this amino acid is substituted. The NL-9-K8A substitution results in an increase in potency, while substitution of the same lysine residue with arginine results in a complete loss of activity. Binding studies should reveal the mechanism of action of the peptide. It is plausible that the peptide is binding DNA and preventing the action of IN or that it is binding the enzyme itself. The NL-9 C2A and C2S substitutions also show a significant loss of peptide inhibitory activity. The corresponding C130 mutants have been shown to have distinct infective dysfunction.[26] This study, as well as unpublished results from our group, shows that the C130 residue has an important role in functional integration of the HIV-1 enzyme. Finally, as mentioned earlier, the ACWW motif seems to be important in enzymatic activity as evidenced by the NL-9 W3A, W4A, W3G, and W4G substitutions, which shows interesting results against wild-type IN. The implication of these and other amino acid residues in successful integration of HIV-1 underscores the importance of studies that identify such residues and investigates possible roles for them.

The α3 and α1 helices of HIV-1 IN, from which the NL-9 and NL-6 peptides are derived, respectively, are on the dimer-

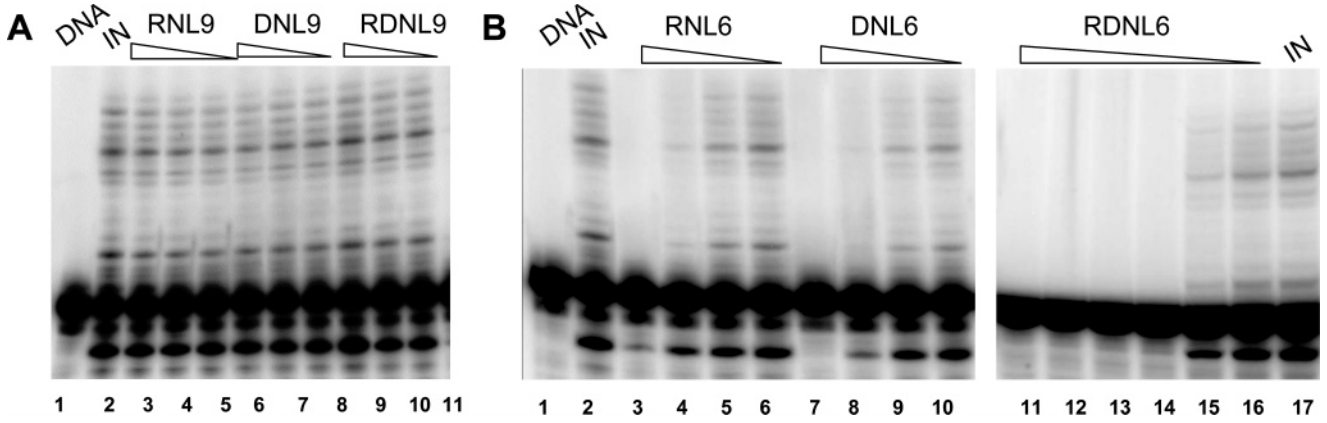

Figure 5. Isomeric forms of NL-6 and NL-9 showing varying activity against wild-type IN. (A) The isomers of NL9 tested against wild-type IN show absolute loss in activity: (lane 1) DNA only; (lane 2) wild-type IN; (lanes 3−5) 333, 111, 37 μM RNL9; (lanes 6−8) 333, 111, 37 μM DNL9; (lanes 9−11) 333, 111, 37 μM RDNL9. (B) Isomers of NL6 show varying activity when compared to parent peptide against wild-type IN: (lane 1) DNA only; (lane 2) wild-type IN only; (lanes 3−6) 333, 111, 37, 12 μM RNL6; (lanes 7−10) 333, 111, 37, 12 μM DNL6; (lanes 11−16) 333, 111, 37, 12, 4, 1.3 μM of RDNL6; (lane 17) wild-type IN only.

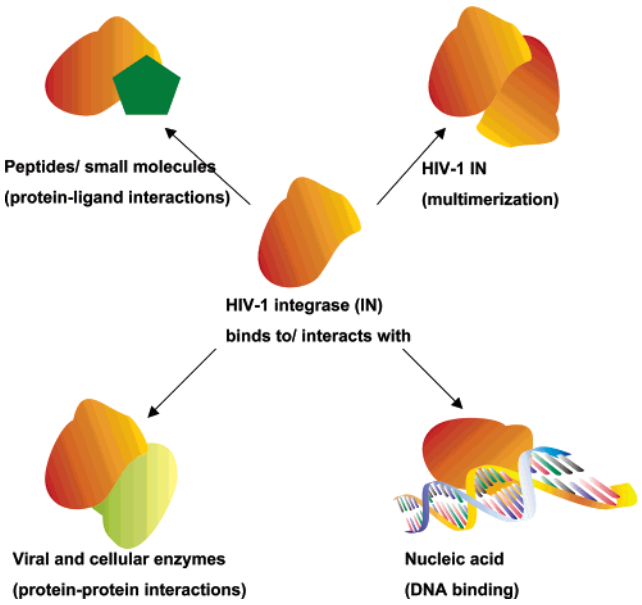

Figure 6. HIV-1 IN binds several biological molecules including other monomers of IN (multimerization), ligands such as small-molecule drugs and peptides, various other viral and cellular proteins, and DNA. Viral proteins such as the matrix protein (MA) and numerous cellular enzymes such as lens epithelium-derived growth factor (LEDGF), IN interacting protein (INI1), and hRad18, a ubiquitin-conjugating enzyme involved in post-replication/translation DNA repair, are examples of proteins with which IN interacts. Inhibitors have been described targeting DNA binding of IN, and studies such as those described in this paper add to the growing body of information toward targeting IN multimerization and its other protein−protein interactions.

ization interface, as shown in Figure 2 within the context of the crystal structure of HIV-1 IN.[19,20,27] It is possible that both these peptides define existing "hot spots" on the enzyme that contain amino acid contacts critical in essential biological interactions of HIV-1 IN, as illustrated by Figure 6. The targeting of such regions on an enzyme provides the template for rational design of successful inhibitors by high-throughput screening, structure-based methods, or in silico studies.[28] For IN, inhibitors to DNA binding have already been identified.[29] The discovery of inhibitors targeting the disruption of other IN interactions that are central to its biological activity will be strengthened by studies such as this, which narrow down areas of interaction to a few important residues. The use of peptides as probes to elucidate critical residues is thus underscored. Indeed, short peptides that bind IN to selectively inhibit one of its catalytic activities (strand transfer) have been identified.[10] It has been proposed that such peptides could be used as tools in elucidating the entire three-dimensional structure of IN.

A comparison of the data in Tables 6 and 7 suggested that the inhibitory activities of these peptides are correlated with the α-helical content, and the orientation of key residue side chains of the peptide is an important factor as well. The best peptide is the retroinverso isomer of NL-6, in which the direction of the sequence is reversed and the chirality of each amino acid residue is inverted. Accordingly, if a retroinverso peptide is superimposed onto the parent peptide in an antiparallel fashion, the overall topology of the side chains is maintained, indicating that the side chain orientations of a peptide and its retroinverso isomer are similar in extended conformations. In addition, the retroinverso peptide possesses the highest percentage of the α-helix conformation, resulting in the best inhibitory activity against HIV-1 IN. The resistance of retroinverso peptides toward proteolytic degradation, compared to the proteolytically susceptible all-L peptide, suggests advantages for the development of novel peptidomimetic IN inhibitors as drug candidates.

Peptide inhibitors of IN have been previously reviewed.[14] While peptides are somewhat unlikely candidates for clinical drug trials because of various issues of stability, delivery, and bioavailability, it must be noted that successful peptide inhibitors to other HIV-1 targets have been described. The fusion inhibitor Fuzeon is one such example already in clinical use, with others being developed.[30] Fuzeon is a peptide that mimics the sequence of the HIV-1 gp41 fusion protein.[31] A peptide inhibitor to virus assembly was also recently identified via phage-display screening of several peptides with similar sequences that bound to a single reactive site within the capsid domain of the Gag protein.[16] In short, potential peptide leads to enzyme inhibition are viable options in drug discovery and cannot be overlooked.

We have developed an innovative and successful approach to provide active IN inhibitors on the basis of the IN sequence itself. Our preliminary data indicate that this strategy yields active leads by testing only a very few derivatives. These data also support our prediction that this study implicates residues essential to HIV-1 IN catalytic activity (unpublished). The peptides NL-6 and NL-9 are expected to serve as leads for further SAR study to find novel IN inhibitors with high selectivity and biological efficacy and also to help further delineate the molecular mechanisms of IN dimerization, protein−protein interactions, nucleic acid binding, and drug interactions.

By extension, this approach could be applied to IN interacting proteins and other therapeutic targets. Studies are underway to assess minimal requirement of reported cellular enzymes that bind to IN and to exploit these as novel drug leads.

Materials and Methods

The physicochemical data of parent peptides and all analogues are summarized in Tables S1−S4 in the Supporting Information.

Materials, Chemicals, and Enzymes. All compounds were dissolved in DMSO, and the stock solutions were stored at −20 °C. The γ[^{32}P]ATP was purchased from either Amersham Biosciences or ICN. The expression systems for wild-type IN were a generous gift from Dr. Robert Craigie, Laboratory of Molecular Biology, NIDDK, NIH, Bethesda, MD.

Preparation of Oligonucleotide Substrates. The oligonucleotides 21top, 5′-GTGTGGAAAATCTCTAGCAGT-3′ and 21bot, 5′-ACTGCTAGAGATTTTCCACAC-3′, were purchased from the Norris Cancer Center Microsequencing Core Facility (University of Southern California) and purified by UV shadowing on polyacrylamide gel. To analyze the extent of 3′-processing and strand transfer using 5′-end labeled substrates, 21top was 5′-end labeled using T_4 polynucleotide kinase (Epicentre, Madison, WI) and γ-[^{32}P]-ATP (Amersham Biosciences or ICN). The kinase was heat-inactivated, and 21-bot was added in 1.5 molar excess. The mixture was heated at 95 °C, allowed to cool slowly at room temperature, and run through a G25 minispin column (USA Scientific) to separate double-double stranded oligonucleotide from unincorporated material.

Integrase Assays. To determine the extent of 3′-processing and strand transfer, wild-type IN was preincubated at a final concentration of 200 nM with the inhibitor in reaction buffer (50 mM NaCl, 1 mM HEPES, pH 7.5, 50 μM EDTA, 50 μM dithiothreitol, 10% glycerol (w/v), 7.5 mM $MnCl_2$, 0.1 mg/mL bovine serum albumin, 10 mM 2-mercaptoethanol, 10% dimethyl sulfoxide, and 25 mM MOPS pH 7.2) at 30 °C for 30 min. An aliquot (5 μL) was electrophoresed on a denaturing 20% polyacrylamide gel (0.09 M Tris-borate, pH 8.3, 2 mM EDTA, 20% acrylamide, 8 M urea). Gels were dried, exposed in a PhosphorImager cassette, analyzed using a Typhoon 8610 variable mode imager (Amersham Biosciences), and quantitated using ImageQuant 5.2. The percent inhibition (*I*) was calculated using the following equation:

$$I\,(\%) = 100 \times \left[1 - \frac{D - C}{N - C}\right]$$

where *C*, *N*, and *D* are the fractions of 21-mer substrate converted to 19-mer (3′-processing product) or strand transfer products for DNA alone, for DNA plus IN, and for DNA plus IN and drug, respectively. The IC_{50} values were determined by plotting the logarithm of drug concentration versus percent inhibition to obtain the concentration that produced 50% inhibition.

Source of Precursor Materials and Analytical Methodologies. Using the fluorenylmethoxycarbonyl (Fmoc) protection strategy, the linear side chain protected peptide NL-1 was synthesized manually on the PAL amide resin (0.151 g, 0.08 mmol, 0.53 mmol/g). The *N*-Fmoc group of the resin was removed with 20% piperidine/DMF (25 min at room temperature) and then coupled with Fmoc-Trp-OH (2.5 equiv) in the presence of DIPCDI (2.5 equiv) and HOBt (2.5 equiv) at room temperature for 2 h. The routine part of the synthesis was carried out manually using Fmoc chemistry (Scheme 1). Side chain protections are as follows: Asn(Trt), Asp(t-Bu), Arg(Pmc), Cys(Trt), Gln(Trt), Glu(t-Bu), His(Trt), Lys(Boc), Ser(tBu), Thr(t-Bu), Tyr(t-Bu). DIPCDI/HOBt activation of N^{α}-protected amino acids was employed for coupling, and 20% piperidine/DMF was used for Fmoc deprotection. The following cocktails were applied for the resin cleavage and side chain deblocking: cleavage system A, TFA/TES/EDT/H_2O (9.4:0.1:0.25:0.25); cleavage system B, TFA/EDT/H_2O (9.5:0.25:0.25); cleavage system C, TFA/TES/H_2O (9.5:0.25:0.25).

This deprotection−coupling cycle was continued until all amino acid residues were linked to the resin. The peptide was cleaved from the resin by using cleavage system A (2 h at room temperature). For isolation of the product, all of the cleavage mixture was evaporated under N_2 to about 3 mL and triturated twice with 20 mL of ice-cold ether. The precipitated crude peptide was dissolved in 20 mL of water and lyophilized. The crude peptides were purified to homogeneity by reverse-phase high-performance liquid chromatography (RP-HPLC). HPLC conditions were as follows: Vydac C18 column (10 mm × 250 mm); solvent A, 0.05% TFA in water; solvent B, 0.05% TFA in 95% acetonitrile in water with gradient indicated below; flow rate, 2.5 mL/min; UV detector, 225, 238, or 254 nm. ESI-MS was performed on a Finnigan LCQ-Deca mass spectrometer. The purity of products was characterized by analytical HPLC and ESI-MS and was more than 98% as determined by HPLC analyses in two diverse systems (system 1, solvent A, 0.05% TFA in water; solvent B, 0.05% TFA in 95% acetonitrile; system 2, solvent A, 0.05% TFA in water; solvent B 0.05% TFA in methol).

Circular Dichroism (CD) Measurements. CD spectra were recorded on a Jasco J-810 spectrometer, using 0.05 cm path length cuvettes at room temperature. Peptides were dissolved at 100 μM in 10 mM PBS, pH 7.2, containing 2,2,2-trifluoroethanol (TFE) (50% v/v). For each peptide sample, the scans of data were collected spanning from 190 to 250 nm in a step size of 0.1 nm. Experimental ellipticity data were converted into molar elliptcities and plotted against wavelength after noise suppression according to the manufacturer's protocol. The α helical content was calculated from CD data based on the method previously described.[24]

H-EEHEKYHSNW-NH_2 (NL-1). The peptide was cleaved from the resin by using cleavage system A (2 h at room temperature). And the product was purified by RP-HPLC (t_R = 10.0 min, gradient 10−15% B over 4 min, 15−35% B over 13 min, UV detector, 225 nm), with an overall yield of 10%. ESI-MS *m/z* ($C_{60}H_{80}N_{18}O_{19}$, calcd 1356.58): 679.8 ([M + 2H]$^{2+}$/2), 690.8 ([M + Na + H]$^{2+}$/2).

H-ASCDKCQLKG-NH_2 (NL-2). Peptide was cleaved from the resin by using cleavage system A (2 h at room temperature) and purified by RP-HPLC (t_R = 12.2 min, gradient 5−22% B over 13 min, UV detector, 225 nm) to provide NL-2 in an overall yield of 30%. ESI-MS *m/z* ($C_{41}H_{74}N_{14}O_{14}S_2$, calcd 1050.5): 1051.9 ([M + H]$^+$), 526.4 ([M + 2H]$^{2+}$/2).

H-HGQVDCSPGIWQLDCTH-NH_2 (NL-3). NL-3 was cleaved from the resin by using cleavage system B (2 h at room temperature) and purified by RP-HPLC (t_R = 14.7 min, gradient 20−60% B over 18 min, UV detector, 238 nm) in an overall yield of 16%. ESI-MS *m/z* ($C_{80}H_{119}N_{25}O_{25}S_2$, calcd 1839.83): 948.0 ([M + 2H]$^{2+}$/2), 959.5 ([M + Na + H]$^{2+}$/2), 967.5 ([M + K + H]$^{2+}$/2).

H-VHVASGY-NH_2 (NL-4). NL-4 was cleaved from the resin by using cleavage system C (2 h at room temperature) and purified by RP-HPLC (t_R = 10.5 min, gradient 10−30% B over 15 min, UV detector, 225 nm) in an overall yield of 24%. ESI-MS *m/z* ($C_{33}H_{50}N_{10}O_9$, calcd 730.38): 731.6 ([M + H]$^+$), 753.6 ([M + Na]$^+$), 366.3 ([M + 2H]$^{2+}$/2).

H-PAETGQET-NH_2 (NL-5). NL-5 was cleaved from the resin by using cleavage system C (2 h at room temperature) and purified by RP-HPLC (t_R = 11.3 min, gradient 10−30% B over 12 min, UV detector, 225 nm) in an overall yield of 15%. ESI-MS *m/z* ($C_{33}H_{54}N_{10}O_{15}$, calcd 830.38): 831.5 ([M + H]$^+$), 853.5 ([M + Na]$^+$), 869.5 ([M + K]$^+$).

H-TAYFLLKLAGRW-NH_2 (NL-6). NL-6 was cleaved from the resin by using cleavage system A (2 h at room temperature) and purified by RP-HPLC (t_R = 12.5 min, gradient 10−25% B over 2 min, 25−40% B over 11 min, UV detector, 254 nm) in an overall yield of 17%. ESI-MS *m/z* ($C_{71}H_{108}N_{18}O_{14}$, calcd 1436.83): 1437.8 ([M + H]$^+$), 1459.7 ([M + Na]$^+$), 719.9 ([M + 2H]$^{2+}$/2).

H-GRWPVKT-NH_2 (NL-7). NL-7 was cleaved from the resin by using cleavage system A (2 h at room temperature) and purified by RP-HPLC (t_R = 9.4 min, gradient 10−15% B over 2 min, 15−35% B over 14 min, UV detector, 238 nm) in an overall yield of

28%. ESI-MS *m/z* ($C_{39}H_{63}N_{13}O_8$, calcd 841.49): 842.7 ($[M + H]^+$), 864.6 ($[M + Na]^+$), 422.4 ($[M + 2H]^{2+}/2$).

H-HTDNGSNF-NH_2 (NL-8). NL-8 was cleaved from the resin by using cleavage system B (2 h at room temperature) and purified by RP-HPLC (t_R = 7.5 min, gradient 10−60% B over 21 min, UV detector, 238 nm) in an overall yield of 28%. ESI-MS *m/z* ($C_{36}H_{51}N_{13}O_{14}$, calcd 889.37): 890.5 ($[M + H]^+$), 913.4 ($[M + Na]^+$), 445.7 ($[M + 2H]^{2+}/2$), 456.7 ($[M + Na + H]^{2+}/2$), 464.7 ($[M + K+H]^{2+}/2$).

H-ACWWAGIKQEF-NH_2 (NL-9). NL-9 was cleaved from the resin by using cleavage system A (2 h at room temperature) and purified by RP-HPLC (t_R = 16.1 min, gradient 10−20% B over 2 min, 20−54% B over 17 min, UV detector, 225 nm) in an overall yield of 11%. ESI-MS *m/z* ($C_{64}H_{88}N_{16}O_{14}S$, calcd 1336.64): 1335.7 ($[M - H]^-$).

H-FGIPYNPQSQ-NH_2 (NL-10). NL-10 was cleaved from the resin by using cleavage system A (2 h at room temperature) and purified by RP-HPLC (t_R = 10.6 min, gradient 5−25% B over 14 min, UV detector, 225 nm) in an overall yield of 11%. ESI-MS *m/z* ($C_{53}H_{76}N_{14}O_{15}$, calcd 1148.56): 1150.7 ($[M + H]^+$), 575.3 ($[M + 2H]^{2+}/2$).

H-ESMNKELKKI-NH_2 (NL-11). NL-11 was cleaved from the resin by using cleavage system A (2 h at room temperature) and purified by RP-HPLC (t_R = 14.2 min, gradient 5−20% B over 16 min, UV detector, 225 nm) in an overall yield of 11%. ESI-MS *m/z* ($C_{52}H_{95}N_{15}O_{16}S$, calcd 1217.68): 610.0 ($[M + 2H]^{2+}/2$).

H-VRDQAEHLKT-NH_2 (NL-12). NL-12 was cleaved from the resin by using cleavage system C (2 h at room temperature) and purified by RP-HPLC (t_R = 12.8 min, gradient 5−20% B over 16 min, UV detector, 225 nm) in an overall yield of 14%. ESI-MS *m/z* ($C_{50}H_{86}N_{18}O_{16}$, calcd 1194.65): 598.4 ($[M + 2H]^{2+}/2$).

H-FIHNFKRK-NH_2 (NL-13). NL-13 was cleaved from the resin by using cleavage system C (2 h at room temperature) and purified by RP-HPLC (t_R = 10.6 min, gradient 10−15% B over 4 min, 15−30% B over 14 min, UV detector, 225 nm) in an overall yield of 23%. ESI-MS *m/z* ($C_{52}H_{81}N_{17}O_9$, calcd 1087.64): 1088.8 ($[M + H]^+$), 545.2 ($[M + 2H]^{2+}/2$)

H-GYSAGERIVD-NH_2 (NL-14). NL-14 was cleaved from the resin by using cleavage system C (2 h at room temperature) and purified by RP-HPLC (t_R = 10.5 min, gradient 10−30% B over 9 min, 30−40% B over 10 min, UV detector, 225 nm) in an overall yield of 24%. ESI-MS *m/z* ($C_{45}H_{72}N_{14}O_{16}$, calcd 1064.53): 1065.9 ($[M + H]^+$), 533.4 ($[M + 2H]^{2+}/2$).

H-WKGPAKLLWK-NH_2 (NL-15). NL-15 was cleaved from the resin by using cleavage system B (2 h at room temperature) and purified by RP-HPLC (t_R = 10.5 min, gradient 10−30% B over 4 min, 30−45% B over 12 min, UV detector, 238 nm) in an overall yield of 40%. ESI-MS *m/z* ($C_{62}H_{96}N_{16}O_{10}$, calcd 1224.75): 1225.9 ($[M + H]^+$), 613.4 ($[M + 2H]^{2+}/2$).

H-VPRRKAKI-NH_2 (NL-16). NL-16 was cleaved from the resin by using cleavage system C (2 h at room temperature) and purified by RP-HPLC (t_R = 10.2 min, gradient 5−20% B over 24 min, UV detector, 225 nm) in an overall yield of 10%. ESI-MS *m/z* ($C_{43}H_{83}N_{17}O_8$, calcd 965.66): 484.0 ($[M + 2H]^{2+}/2$).

Acknowledgment. The work in Y.-Q.L.'s laboratory was supported by funds from NSFC (Grant No. 30200351) and Shanghai Municipal Committee of Science and Technology (Grant Nos. 03DZ19219 and 02QB14056). The work in N.N.'s laboratory was supported by funds from GlaxoSmithKline Drug Discovery and Development Award.

Supporting Information Available: CD, MS, and HPLC data and conditions. This material is available free of charge via the Internet at http://pubs.acs.org.

References

(1) Engelman, A.; Mizuuchi, K.; Craigie, R. HIV-1 DNA integration: mechanism of viral DNA cleavage and DNA strand transfer. *Cell* **1991**, *67*, 1211−1121.

(2) Asante-Appiah, E.; Skalka, A. M. HIV-1 integrase: structural organization, conformational changes, and catalysis. *Adv. Virus Res.* **1999**, *52*, 351−369.

(3) Brown, P. O. Integration. In *Retroviruses*; Coffin, J. C., Hughes, S. H., Varmus, H. E., Eds.; Cold Spring Harbor Press: Plainview, NY, 1999.

(4) Van Maele, B.; Debyser, Z. HIV-1 integration: an interplay between HIV-1 integrase, cellular and viral proteins. *AIDS Rev.* **2005**, *7* (1), 26−43.

(5) Tasara, T.; Maga, G.; Hottiger, M. O.; Hubscher, U. HIV-1 reverse transcriptase and integrase enzymes physically interact and inhibit each other. *FEBS Lett.* **2001**, *507* (1), 39−44.

(6) Bushman, F. D.; Engelman, A.; Palmer, I.; Wingfield, P.; Craigie, R. Domains of the integrase protein of human immunodeficiency virus type 1 responsible for polynucleotidyl transfer and zinc binding. *Proc. Natl. Acad. Sci. U.S.A.* **1993**, *90* (8), 3428−3432.

(7) Maroun, R. G.; Gayet, S.; Benleulmi, M. S.; Porumb, H.; Zargarian, L.; Merad, H.; Leh, H.; Mouscadet, J. F.; Troalen, F.; Fermandjian, S. Peptide inhibitors of HIV-1 integrase dissociate the enzyme oligomers. *Biochemistry* **2001**, *40* (46), 13840−13848.

(8) Lutzke, R. A. P.; Eppens, N. A.; Weber, P. A.; Houghten, R. A.; Plasterk, R. H. A. Identification of a hexapeptide inhibitor of the human immunodeficiency virus integrase protein by using a combinatorial chemical library. *Proc. Natl. Acad. Sci. U.S.A.* **1995**, *92*, 11456−11460.

(9) de Soultrait, V. R.; Caumont, A.; Parissi, V.; Morellet, N.; Ventura, M.; Lenoir, C.; Litvak, S.; Fournier, M.; Roques, B. A novel short peptide is a specific inhibitor of the human immunodeficiency virus type 1 integrase. *J. Mol. Biol.* **2002**, *318* (1), 45−58.

(10) Desjobert, C.; de Soultrait, V. R.; Faure, A.; Parissi, V.; Litvak, S.; Tarrago-Litvak, L.; Fournier, M. Identification by phage display selection of a short peptide able to inhibit only the strand transfer reaction catalyzed by human immunodeficiency virus type 1 integrase. *Biochemistry* **2004**, *43* (41), 13097−13105.

(11) Oz Gleenberg, I.; Avidan, O.; Goldgur, Y.; Herschhorn, A.; Hizi, A. Peptides derived from the reverse transcriptase of human immunodeficiency virus type 1 as novel inhibitors of the viral integrase. *J. Biol. Chem.* **2005**, *280* (23), 21987−21996.

(12) Zhao, L.; O'Reilly, M. K.; Shultz, M. D.; Chmielewski, J. Interfacial peptide inhibitors of HIV-1 integrase activity and dimerization. *Bioorg. Med. Chem. Lett.* **2003**, *13* (6), 1175−1177.

(13) Maroun, R. G.; Krebs, D.; Roshani, M.; Porumb, H.; Auclair, C.; Troalen, F.; Fermandjian, S. Conformational aspects of HIV-1 integrase inhibition by a peptide derived from the enzyme central domain and by antibodies raised against this peptide. *Eur. J. Biochem.* **1999**, *260* (1), 145−155.

(14) de Soultrait, V. R.; Desjobert, C.; Tarrago-Litvak, L. Peptides as new inhibitors of HIV-1 reverse transcriptase and integrase. *Curr. Med. Chem.* **2003**, *10*, 1765−1778.

(15) Kilby, J. M.; Hopkins, S.; Venetta, T. M.; DiMassimo, B.; Cloud, G. A.; Lee, J. Y.; Alldredge, L.; Hunter, E.; Lambert, D.; Bolognesi, D.; Matthews, T.; Johnson, M. R.; Nowak, M. A.; Shaw, G. M.; Saag, M. S. Potent suppression of HIV-1 replication in humans by T-20, a peptide inhibitor of gp41-mediated virus entry. *Nat. Med.* **1998**, *4* (11), 1302−1307.

(16) Sticht, J.; Humbert, M.; Findlow, S.; Bodem, J.; Muller, B.; Dietrich, U.; Werner, J.; Krausslich, H. G. A peptide inhibitor of HIV-1 assembly in vitro. *Nat. Struct. Mol. Biol.* **2005**, *12* (8), 671−677.

(17) Neamati, N.; Marchand, C.; Pommier, Y. HIV-1 integrase inhibitors: past, present, and future. *Adv. Pharmacol.* **2000**, *49*, 147−165.

(18) Engelman, A. In vivo analysis of retroviral integrase structure and function. *Adv. Virus Res.* **1999**, *52*, 411−426.

(19) Dyda, F.; Hickman, A. B.; Jenkins, T. M.; Engelman, A.; Craigie, R.; Davies, D. R. Crystal structure of the catalytic domain of HIV-1 integrase: similarity to other polynucleotidyl transferases. *Science* **1994**, *266* (5193), 1981−1986.

(20) Wang, J. Y.; Ling, H.; Yang, W.; Craigie, R. Structure of a two-domain fragment of HIV-1 integrase: implications for domain organization in the intact protein. *EMBO J.* **2001**, *20* (24), 7333−7343.

(21) Chorev, M.; Goodman, M. Recent developments in retro peptides and proteins—an ongoing topochemical exploration. *Trends Biotechnol.* **1995**, *13* (10), 438−445.

(22) Fletcher, M. D.; Campbell, M. M., Partially modified retro-inverso peptides: development, synthesis, and conformational behavior. *Chem. Rev.* **1998**, *98*, 8 (2), 763−796.

(23) Sakurai, K.; Chung, H. S.; Kahne, D. Use of a retroinverso p53 peptide as an inhibitor of MDM2. *J. Am. Chem. Soc.* **2004**, *126* (50), 16288−16289.

(24) Forood, B.; Feliciano, E. J.; Nambiar, K. P. Stabilization of alpha-helical structures in short peptides via end capping. *Proc. Natl. Acad. Sci. U.S.A.* **1993**, *90* (3), 838−842.

(25) Mazumder, A.; Neamati, N.; Pilon, A. A.; Sunder, S.; Pommier, Y. Chemical trapping of ternary complexes of human immunodeficiency virus type 1 integrase, divalent metal, and DNA substrates containing an abasic site. Implications for the role of lysine 136 in DNA binding. *J. Biol. Chem.* **1996**, *271* (44), 27330−27338.
(26) Zhu, K.; Dobard, C.; Chow, S. A. Requirement for integrase during reverse transcription of human immunodeficiency virus type 1 and the effect of cysteine mutations of integrase on its interactions with reverse transcriptase. *J. Virol.* **2004**, *78* (10), 5045−5055.
(27) Bujacz, G.; Alexandratos, J.; Qing, Z. L.; Clement-Mella, C.; Wlodawer, A. The catalytic domain of human immunodeficiency virus integrase: ordered active site in the F185H mutant. *FEBS Lett.* **1996**, *398* (2−3), 175−178.
(28) Neamati, N. Structure-based HIV-1 integrase inhibitor design: a future perspective. *Expert Opin. Invest. Drugs* **2001**, *10* (2), 281−296.
(29) Neamati, N.; Mazumder, A.; Sunder, S.; Owen, J. M.; Tandon, M.; Lown, J. W.; Pommier, Y. Highly potent synthetic polyamides, bisdistamycins, and lexitropsins as inhibitors of human immunodeficiency virus type 1 integrase. *Mol. Pharmacol.* **1998**, *54* (2), 280−290.
(30) Williams, I. G. Enfuvirtide (Fuzeon): the first fusion inhibitor. *Int. J. Clin. Pract.* **2003**, *57* (10), 890−897.
(31) Wild, C. T.; Shugars, D. C.; Greenwell, T. K.; McDanal, C. B.; Matthews, T. J. Peptides corresponding to a predictive alpha-helical domain of human immunodeficiency virus type 1 gp41 are potent inhibitors of virus infection. *Proc. Natl. Acad. Sci. U.S.A.* **1994**, *91* (21), 9770−9774.

JM060307U